

Structural basis for α -tubulin-specific and modification state-dependent glutamylation

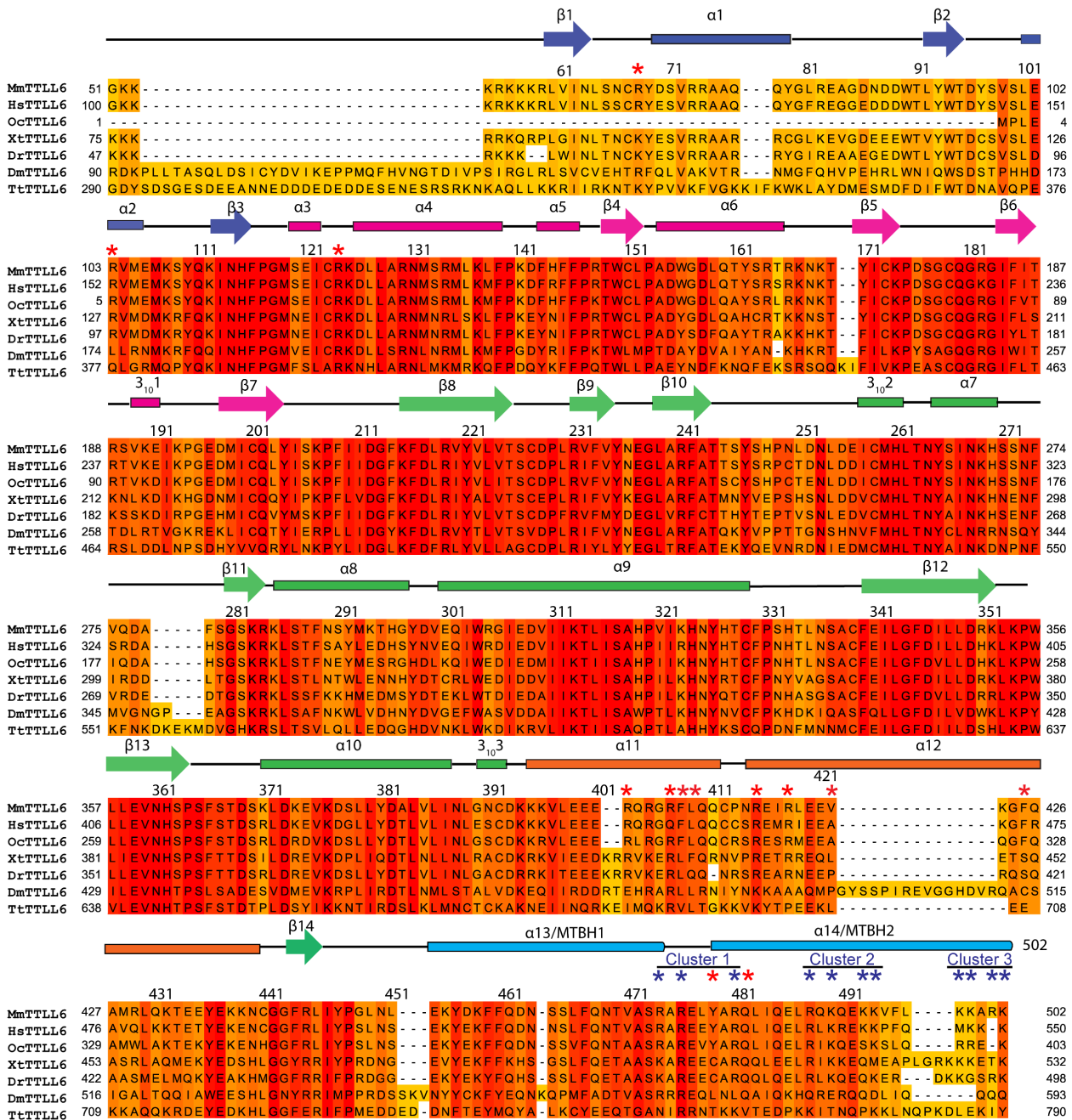
In the format provided by the authors and unedited

Supplementary Table 1. Cryo-EM data collection statistics.

Data collection			
Microscope	Talos Arctica		
Detector	K2 Summit		
Data collection software	Leginon		
Nominal magnification	36,000x		
Voltage (kV)	200		
Electron exposure ($e^-/\text{\AA}^2$)	42		
Exposure rate ($e^-/\text{pixel/s}$)	5.5		
Defocus range (μm)	-1.0 to -2.0		
Pixel size (\AA)	1.15		
Time per frame (s)	0.250		
Total exposure time (s)	9.75		
Frames per movie	39		
Movies collected	2,771		
Image processing			
	Microtubule-TTLL6 map (EMDB-41018)	TTLL6 focused map (EMDB-41022)	Composite map (EMDB-41090)
Symmetry imposed	C1	C1	C1
Initial particle images	59,044(microtubule segments)	392,289	
Final particle images	392,289(protofilament particles)	151,716	
Map resolution (\AA)	3.6	7.2	3.7
FSC threshold	0.143	0.143	0.143
Map resolution range (\AA)	3 to 14	5 to 14	3 to 14
Map sharpening B factor (\AA^2)		-18	

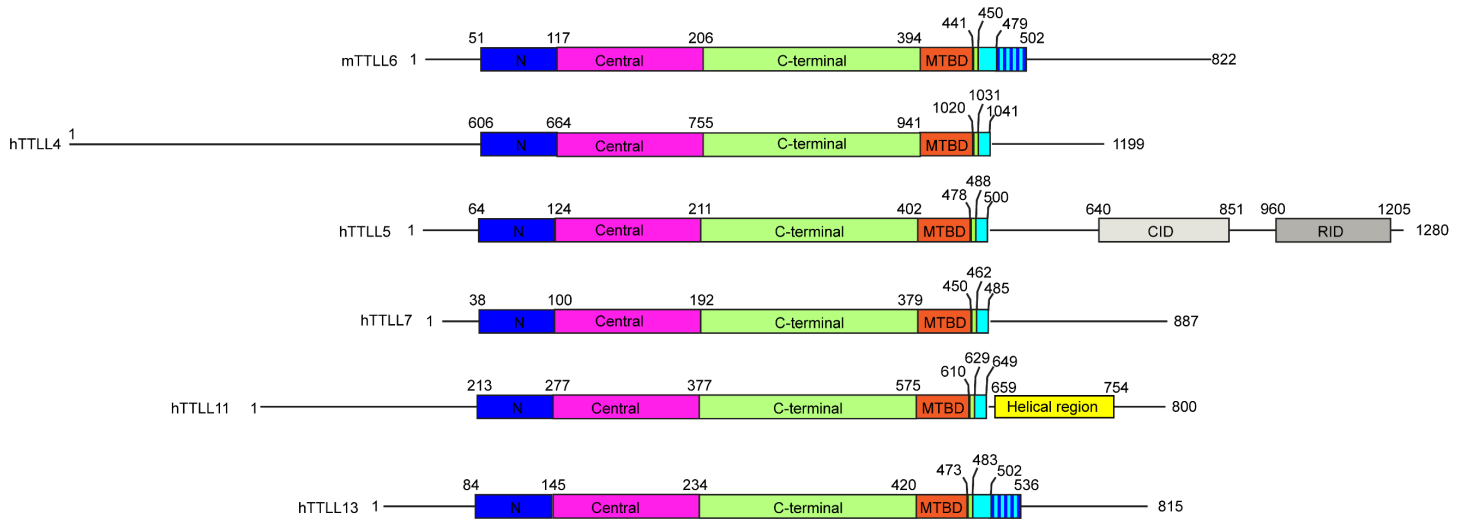
Supplementary Table 2. Model refinement and validation statistics.

Two protofilament microtubule-TTL6 model (EMDB-41018) (PDB 8T42)	
Atomic modeling refinement packages	Phenix, Coot
Initial model used (PDB code)	6VZU, 5N5N
Model resolution (Å)	3.5
FSC threshold	0.143
Model composition	
Non-hydrogen atoms	13,864
Protein residues	1,752
Ligands	2 GTP; 2 GMPCPP; 4 Mg ²⁺
<i>B</i> factors (Å ²)	
Protein	99.3
Ligand	95.8
R.M.S. Deviations	
Bond lengths (Å)	0.007
Bond angles (°)	1.434
Validation	
MolProbity score	1.46 (100 th percentile)
Clashscore	3.82 (100 th percentile)
Poor rotamers	2 (0.13%)
EMRinger score	2.40
Ramachandran plot	
Favored	1,678 (95.8%)
Allowed	74 (4.2%)
Disallowed	0
Rama-Z score	
whole	-1.35
helix	0.12
sheet	-2.25
loop	-1.29
Model vs. Data	
CC(volume)	0.82
CC(mask)	0.82



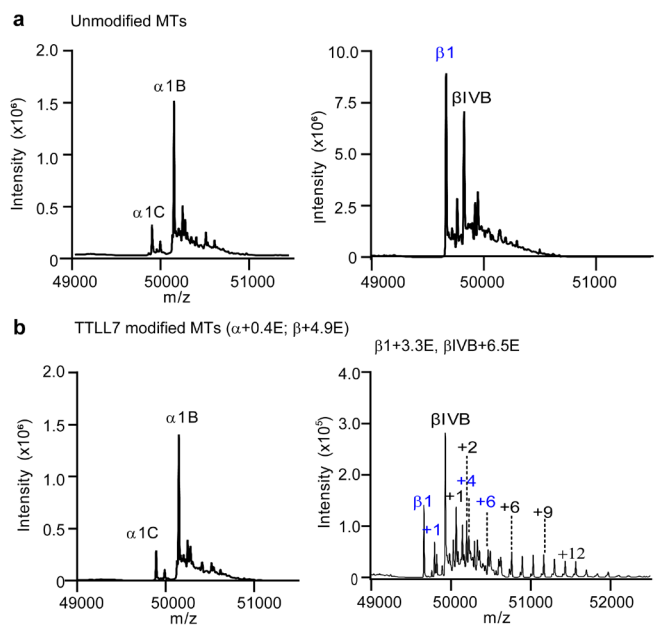
Supplementary Fig. 1. TLL6 sequence conservation.

TLL6 sequences belonging to Mm- *Mus musculus*, Hs- *Homo sapiens*, Oc- *Oryctolagus cuniculus*, Xt- *Xenopus tropicalis*, Dr- *Danio rerio*, Dm- *Drosophila melanogaster*, Tt- *Tetrahymena thermophila*, were aligned using Clustal omega in Jalview¹. Secondary structure elements are indicated above the corresponding sequence. Residues in the cationic clusters in the MTBH1-2 are marked with blue asterisks. Other residues important for microtubule recognition are marked using a red asterisk on top.



Supplementary Fig. 2. Structure based sequence-based alignment showing the absence of a cationic MTBH2 in TLL initiases, TLL4 and 5.

Domain organization of autonomous TLL glutamylases with TLL6 shown at the top followed by TLL4, 5, 7, 11 and 13 showing the lack of a cationic MTBH2 in TLL4, 5, 7 and 11. TLL 4, 5 and 7 prefer to initiate glutamate chains²⁻⁶. The MTBH2 is clearly missing in TLL4 and 5. TLL7 has an MTBH2 which misses critical positively charged residue and folds against its core². TLL13 has a clearly defined MTBH1-2. Unlike TLL6 and 13, TLL11 lacks a single helical feature similar to MTBH2 but its MTBH1 is followed by a helical bundle (highlighted in yellow), with positively-charged residues, whose function could be analogous to MTBH2. The N-, central-, C- and MTBD domains are shown in blue, magenta, green and orange, respectively. MTBH1 is shown in cyan and the cationic MTBH2 in TLL6 is shown in cyan with blue stripes indicating the location of arginine and lysine rich regions. The cofactor interaction domain (CID) and receptor interaction domain (RID) of TLL5 are shown in grey.



Supplementary Fig. 3. TLL7 glutamylated microtubules.

a, b. LC-MS spectra of unmodified (a) and TLL7 glutamylated microtubules used in TIRF-based microtubule binding assays in Figures 7a-c (b) (Methods). Tubulin isotypes and the number of glutamates post-translationally added by TLL7 are indicated on top. The mean number of glutamates added to each tubulin isotype after TLL7 treatment is shown above the spectra and was calculated as described previously^{7,8}.

References:

1. Waterhouse, A.M., Procter, J.B., Martin, D.M., Clamp, M., and Barton, G.J. (2009). Jalview Version 2--a multiple sequence alignment editor and analysis workbench. *Bioinformatics* 25, 1189-1191. 10.1093/bioinformatics/btp033.
2. Garnham, C.P., Vemu, A., Wilson-Kubalek, E.M., Yu, I., Szyk, A., Lander, G.C., Milligan, R.A., and Roll-Mecak, A. (2015). Multivalent Microtubule Recognition by Tubulin Tyrosine Ligase-like Family Glutamylases. *Cell* 161, 1112-1123. 10.1016/j.cell.2015.04.003.
3. Janke, C., Rogowski, K., Wloga, D., Regnard, C., Kajava, A.V., Strub, J.M., Temurak, N., van Dijk, J., Boucher, D., van Dorsselaer, A., et al. (2005). Tubulin polyglutamylase enzymes are members of the TTL domain protein family. *Science* 308, 1758-1762. 10.1126/science.1113010.
4. Mahalingan, K.K., Keith Keenan, E., Strickland, M., Li, Y., Liu, Y., Ball, H.L., Tanner, M.E., Tjandra, N., and Roll-Mecak, A. (2020). Structural basis for polyglutamate chain initiation and elongation by TTLL family enzymes. *Nat Struct Mol Biol* 27, 802-813. 10.1038/s41594-020-0462-0.
5. Mukai, M., Ikegami, K., Sugiura, Y., Takeshita, K., Nakagawa, A., and Setou, M. (2009). Recombinant mammalian tubulin polyglutamylase TTLL7 performs both initiation and elongation of polyglutamylation on beta-tubulin through a random sequential pathway. *Biochemistry* 48, 1084-1093. 10.1021/bi802047y.
6. van Dijk, J., Rogowski, K., Miro, J., Lacroix, B., Edde, B., and Janke, C. (2007). A targeted multienzyme mechanism for selective microtubule polyglutamylation. *Mol Cell* 26, 437-448. 10.1016/j.molcel.2007.04.012.
7. Szczesna, E., Zehr, E.A., Cummings, S.W., Szyk, A., Mahalingan, K.K., Li, Y., and Roll-Mecak, A. (2022). Combinatorial and antagonistic effects of tubulin glutamylation and glycylation on katanin microtubule severing. *Dev Cell* 57, 2497-2513 e2496. 10.1016/j.devcel.2022.10.003.
8. Valenstein, M.L., and Roll-Mecak, A. (2016). Graded Control of Microtubule Severing by Tubulin Glutamylation. *Cell* 164, 911-921. 10.1016/j.cell.2016.01.019.